Research Article | Vol. 25, No. 12 | 12 Jun 2017 | OPTICS EXPRESS 13903
Optics EXPRESS

Nanoparticle doping for high power fiber lasers at eye-safer wavelengths

COLIN C. BAKER,[1,*] E. JOSEPH FRIEBELE,[2] ASHLEY A. BURDETT,[3] DANIEL L. RHONEHOUSE,[3] JAKE FONTANA,[1] WOOHONG KIM,[1] STEVEN R. BOWMAN,[1] L. BRANDON SHAW,[1] JASBINDER SANGHERA,[1] JUN ZHANG,[4] RADHA PATTNAIK,[4] MARK DUBINSKII,[4] JOHN BALLATO,[5] COURTNEY KUCERA,[5] AMBER VARGAS,[5] ALEXANDER HEMMING,[6] NIKITA SIMAKOV,[6] AND JOHN HAUB[6]

[1]*Naval Research Laboratory, 4555 Overlook Ave. SW, Washington, DC 20375, USA*
[2]*Sotera Defense Solutions,7230 Lee DeForest Drive, Suite 100, Columbia, MD 21046, USA*
[3]*University Research Foundation, 6411 Ivy Lane, Suite 110, Greenbelt MD 20770, USA*
[4]*Army Research Laboratory, 2800 Powder Mill Road, Adelphi, MD 20783, USA*
[5]*Department of Materials Science and Engineering and the Center for Optical Materials Science and Engineering Technologies (COMSET), Clemson University, Anderson, SC 29625, USA*
[6]*Defence Science & Technology Group, Edinburgh, SA 5111, Australia*
[*]*colin.baker@nrl.navy.mil*

Abstract: A nanoparticle (NP) doping technique was developed for fabricating erbium (Er)- and holmium (Ho)-doped silica-based optical fibers for high energy lasers. Slope efficiencies in excess of 74% were realized for Er NP doping in a single mode fiber based master oscillator power amplifier (MOPA) and 53% with multi-Watt-level output in a resonantly cladding-pumped power oscillator laser configuration based on a double-clad fiber. Cores comprising Ho doped LaF_3 and Lu_2O_3 nanoparticles exhibited slope efficiencies as high as 85% at 2.09 μm in a laser configuration. To the best of the authors' knowledge, this is the first report of a holmium nanoparticle doped fiber laser as well as the highest efficiency and power output reported from an erbium nanoparticle doped fiber laser.

OCIS codes: (140.3510) Lasers, fiber; (140.3500) Lasers, erbium; (160.4236) Nanomaterials.

References and links

1. J. A. Zuclich, D. A. Gagllano, F. Cheney, B. E. Stuck, H. Zwick, P. Edsall, and D. J. Lund, "Ocular effects of penetrating IR laser wavelengths," Proc. SPIE **2391**, 112–125 (1995).
2. J. E. Townsend, S. B. Poole, and D. N. Payne, "Solution doping technique for fabrication of rare-earth-doped optical fibres," Electron. Lett. **23**(7), 329–331 (1987).
3. W. J. Miniscalco, "Optical and electronic properties of rare earth ions in glasses," in *Rare-Earth-Doped Fiber Lasers and Amplifiers,* 2nd ed., Michel J.F. Digonnet ed. (Marcel Dekker, Inc. 2001).
4. A. Pastouret, C. Gonnet, C. Collet, O. Cavani, E. Burov, C. Chanéac, A. Carton, and J.-P. Jolivet, "Nanoparticle Doping Process for Improved Fibre Amplifiers and Lasers," Proc. SPIE **7195**, 71951X (2009).
5. D. Boivin, A. Pastouret, E. Burov, C. Gonnet, O. Cavani, S. Lempereur, and P. Sillard, "Performance Characterization of New Erbium-doped Fibers using MCVD Nanoparticle Doping Process," Proc. SPIE **7914**, 791423 (2011).
6. J. P. Jolivet, C. Froidefond, A. Pottier, C. Cheneac, S. Cassaignon, E. Tronc, and P. Euzen, "Size tailoring of oxide nanoparticles by precipitation in aqueous medium. A semi-quantitative modelling," J. Mater. Chem. **14**(21), 3281–3288 (2004).
7. C. Kucera, B. Kokuoz, D. Edmondson, D. Griese, M. Miller, A. James, W. Baker, and J. Ballato, "Designer emission spectra through tailored energy transfer in nanoparticle-doped silica preforms," Opt. Lett. **34**(15), 2339–2341 (2009).
8. I. Kasik, P. Peterka, J. Mrazek, and P. Honzatko, "Silica Optical Fibers Doped with Nanoparticles for Fiber Lasers and Broadband Sources," Curr. Nanosci. **12**(3), 277–290 (2016).
9. O. Podrazky, I. Kasik, M. Pospisilova, and V. Matejec, "Use of nanoparticles for preparation of rare-earth doped silica fibers," Phys. Status Solidi., C Curr. Top. Solid State Phys. **6**(10), 2228–2230 (2009).
10. W. Blanc, B. Dussardier, G. Monnom, R. Peretti, A.-M. Jurdyc, B. Jacquier, M. Foret, and A. Roberts, "Erbium emission properties in nanostructured fibers," Appl. Opt. **48**(31), G119–G124 (2009).

#292876 https://doi.org/10.1364/OE.25.013903
Journal © 2017 Received 19 Apr 2017; revised 17 May 2017; accepted 18 May 2017; published 9 Jun 2017

Optics EXPRESS

11. J. Koponen, L. Petit, T. Kokki, V. Aallos, J. Paul, and H. Ihalainen, "Progress in direct nanoparticle deposition for the development of the next generation fiber lasers," Opt. Eng. **50**(11), 111605 (2011).
12. M. J. Weber, "Probabilities for Radiative and Nonradiative Decay of Er^{3+} in LaF_3," Phys. Rev. **157**(2), 262–272 (1967).
13. O. Humbach, H. Fabian, U. Grzesik, U. Haken, and W. Heitmann, "Analysis of OH absorption bands in synthetic silica," J. Non-Cryst. Solids **203**, 19–26 (1996).
14. E. J. Friebele, C. G. Askins, J. R. Peele, B. M. Wright, N. J. Condon, S. O'Connor, C. G. Brown, and S. R. Bowman, "Ho-Doped Fiber for High Energy Laser Applications," Proc. SPIE **8961**, 896120 (2014).
15. E. J. Friebele, C. G. Askins, B. A. Marcheschi, C. C. Baker, W. Kim, J. R. Peele, J. Zhang, R. K. Pattnaik, L. D. Merkle, and M. Dubinskii, "Nanoparticle Doping for Improved Power Scaling of Resonantly-Pumped, Yb-Free Er-Doped Fiber Lasers" in SPIE Defense, Security and Sensing Conference, 9081–7 (2014).
16. E. J. Friebele, C. C. Baker, C. G. Askins, J. P. Fontana, M. P. Hunt, J. R. Peele, B. A. Marcheschi, E. Oh, W. Kim, J. Sanghera, J. Zhang, R. K. Pattnaik, L. D. Merkle, and M. Dubinskii, "Erbium nanoparticle-doped fibers for efficient, resonantly-pumped Er-doped fiber lasers," Proc. SPIE **9344**, 934412 (2015).
17. C. C. Baker, E. J. Friebele, C. G. Askins, M. P. Hunt, J. P. Fontana J. R. Peele, B. A. Marcheschi, W. Kim, J. Sanghera, J. Zhang, R. K. Pattnaik, L. D. Merkle, M. Dubinskii, Y. Chen, I. A. Dajani, and C. Mart, "Nanoparticle Doping for Improved Er-doped Fiber Lasers," Proc. SPIE **9728**, 97280T (2016).
18. C. C. Baker, E. J. Friebele, C. G. Askins, B. A. Marcheschi, J. R. Peele, W. Kim, J. S. Sanghera, J. Zhang, M. Dubinskii, and Y. Chen, "Nanoparticle doping for high power lasers at eye-safer wavelengths," Lasers Congress 2016 (ASSL, LSC, LAC), OSA Technical Digest (online) (Optical Society of America, 2016), paper AM3A.1.
19. P. R. Diamente, M. Raudsepp, and F. C. van Veggel, "Dispersible Tm^{3+}-doped nanoparticles that exhibit strong 1.47 μm photoluminescence," Adv. Funct. Mater. **17**(3), 363–368 (2007).

1. Introduction

Highlighted in this work are recent accomplishments in nanoparticle doping of high power fiber lasers operating at "eye-safer" wavelengths. Both erbium and holmium doped fiber lasers are attractive candidates for high energy lasers (HELs) used in directed energy applications because they operate at wavelengths that are both safer to the eye and in a high atmospheric transmission window. Diffuse and low intensity parasitic reflections from dust, aerosols, or the target itself can be focused onto the retina with a gain of $>10^4$ for wavelengths <1.4 μm [1]. Though technically not eye-safe due to the high powers employed, some degree of laser safety can be gained by operation at wavelengths >1.4 μm since the cornea, lens, vitreous- and aqueous-humor absorb the light and reduce the potential chance of retinal damage. In addition, the high atmospheric transmission windows exists between ~1.5-1.75μm and beyond 2.1μm.

In nanoparticle doping of silica fibers, the rare earth ions are encapsulated within the nanoparticle host. Here the rare earth ions are ideally separated from one another in the host, and are thereby isolated from the influence of the silica lattice. In order to understand why this is needed, a brief review of the process and issues associated with conventional solution doping of silica with erbium and holmium is provided.

Fabrication of rare earth (RE^{3+})-doped optical fibers is typically performed by solution doping [2] where salts of the rare earth ion, such as $ErCl_3$ and Al (added to decrease clustering of the REs) are dissolved in a solvent and introduced into a layer of porous silica "soot" that is subsequently dried and consolidated to form the fiber core. However, there is no mechanism for controlling the molecular environment about the RE^{3+} ions when solution doped into the homogeneous glass. This particularly presents problems for erbium; in spite of the addition of Al, Er^{3+} ions tend to cluster. As the neighboring ion-ion distance decreases, the probability of ion-ion interaction increases, which results in excited state energy transfer processes, such as upconversion and quenching, which greatly reduce laser efficiency.

Upconversion in Er^{3+} doped fibers is manifested when two excited ions, close in proximity, interact, with one ion transferring its energy to the other, leaving itself in the ground state ($^4I_{15/2}$) and the other in a higher lying energy state; e.g., the $^4I_{9/2}$ level. In SiO_2 glass, the $^4I_{9/2}$ state quickly relaxes through multiphonon relaxation back to the $^4I_{13/2}$ state, resulting in the generation of heat [3]. This is an especially detrimental process for HELs because of the potentially large amount of heat generated and the decrease in lasing efficiency.

Optics EXPRESS

Ideally, for substantial laser power scaling, the concentration of laser active RE^{3+} ions in the fiber must be increased, both to minimize the active fiber length in order to reduce nonlinear processes and to enable clad pumping where the effective RE^{3+} absorption is diluted by the ratio of the core to pump clad areas. While this is generally not a problem for Yb^{3+} doping with its simple two level structure, it is a great concern for other RE^{3+} ions that have more complex energy level structures and dynamics. For these dopants, increased RE^{3+} concentrations can facilitate the unwanted excited state energy transfer processes since the RE^{3+} ions are, on average, closer to each other in the doped glass.

Nanoparticle doping can be used to minimize these effects since the nanoparticles can serve to isolate the dopant from the SiO_2 glass. Foundational work in NP doping was performed in erbium doped fibers, where Er^{3+}-doped boehmite (Er:AlOOH) nanoparticles were synthesized by the aqueous co-precipitation of Er and Al precursors; the particles were ripened and underwent subsequent thermal processing to form stable Er:Al_2O_3 NPs [4–6]. Nanoparticle doping using LaF_3 hosts was achieved by Kucera et al [7] where tailored emission spectra were demonstrated, indicating effective isolation of RE^{3+} ions. Several other research groups have utilized aspects of nanoparticle doping in various forms (for a review see [8]). Techniques include adding commercially-available Al_2O_3 and Er_2O_3 nanoparticles into a fiber as a co-dopant mixture [9], in situ growth of nanoparticles in the preform [10], and Direct Nanoparticle Deposition (DND), where separate rare earth oxide and SiO_2 nanoparticle mixtures are flame-sprayed in an outside vapor deposition technique [11]. Note, however, in these techniques it is not clear if processes where oxide nanoparticles are either mixed, or grown in situ, result in effective isolation of the Er^{3+} ions in the nanoparticle network, which is what this work seeks to do.

The silica lattice of the fiber can also be detrimental to achieving optimum RE^{3+} properties. The fluorescence lifetime of a RE^{3+} transition is governed by the sum of all probabilities for both radiative and non-radiative relaxation pathways [12]. The highest energy phonon for SiO_2 is at 1100cm^{-1}, which is relatively large in comparison to the energy spacing between many RE^{3+} excited states. It is particularly detrimental for long-wavelength transitions, such as the $^5I_7 \rightarrow {}^5I_8$ transition near 2.1 μm in Ho^{3+}, which non-radiatively couples energy to the glass host through a multiphonon relaxation of the ions, which occurs at a much greater rate than radiative relaxation. Because phonon quenching reduces fluorescence lifetimes for RE^{3+} dopants, lasing efficiency is concomitantly reduced. The probability for multiphonon relaxation decreases exponentially with the number of phonons required to bridge the energy gap between states. As a general rule of thumb the process is favorable for transitions that would require <5 phonons to bridge the energy gap [12]. Exemplifying this, take the $^5I_7 \rightarrow {}^5I_8$ transition of Ho^{3+} near 2 μm, which has an energy difference of ~5000 cm^{-1}, which is <5 phonons with 1100 cm^{-1} energy in silica, so that this multiphonon quenching results in a reduced radiative lifetime. Since the combination of radiative and non-radiative processes results in decreased lifetimes for RE^{3+} ions in high phonon energy hosts for longer wavelengths transitions, hosts with a smaller phonon energy than SiO_2 are desirable. While employing an alternate glass host is possible to achieve lower multiphonon quenching and higher efficiency, typically these low phonon glasses are difficult to fabricate and have higher losses than silica. Alternately, as is the focus here, the local environment, hence phonon energy, about the RE^{3+} can be tailored by incorporating it within a suitable nanoparticle that is dispersed into the silica matrix thus achieving low loss and high strength from the silica host with the reduced phonon energy of the NP. This includes nanoparticle hosts such as LaF_3 with a maximum phonon energy of ~350 cm^{-1} and Lu_2O_3 with a maximum phonon energy of 430 cm^{-1}. Even Al_2O_3 with its maximum phonon energy of 870 cm^{-1} is preferred over direct interaction between the RE^{3+} and the SiO_2 matrix.

Another loss mechanism that is especially significant for holmium-doped fibers is OH^- absorption. It has been estimated that the loss associated from OH- absorption is 0.06 dB/m-ppm^{-1} OH at 1.38 μm [13]. OH incorporation occurs during preform fabrication from solution

Optics EXPRESS

doping and OH adsorption by the silica soot and thus gives an added complication for holmium doping. It is essential to eliminate as much OH^- as possible, ideally keeping its concentration below 1 ppm [13,14]. Therefore, alternative techniques for holmium doping must include considerations for reducing the OH^- contamination and extensive drying to remove any residual OH. In addition to OH- absorption, the potential exists for resonant energy transfer from the excited Ho^{3+} ion to an OH^- impurity center. Since OH^- is effectively incorporated into silica through an Si-OH bond, encapsulating the Ho^{3+} ion into the nanoparticle should effectively isolate the excited $Ho^{3+}$from being quenched due to this mechanism.

Specifically, in this work, Er^{3+} - or Ho^{3+} - nanoparticles of Al_2O_3, LaF_3 and Lu_2O_3, have been synthesized and doped into conventional HEL silica-based preforms from which we have drawn high quality fibers with low background loss [15–18]. Reported here are Er nanoparticle doping concentrations that are higher than previously reported. Also reported, for the first time to our knowledge, are high amplifier and laser slope efficiencies using fibers based on this doping technique. Also reported are Ho^{3+} NP doped fibers, with which the demonstration of lasing is first reported to our knowledge.

2. Experiment

Several RE^{3+}/NP systems were synthesized in this work. The Er-doped Al_2O_3 nanoparticles were synthesized using a co-precipitation technique from aluminum (III) nitrate hydrate (Sigma-Aldrich, 99.999%) and erbium chloride (Alfa-Aesar, 99.9%). Various Al and Er molarities in the precursor solutions were investigated with the aim of obtaining molar ratios of Al:Er in the range between 10:1 and 200:1. Here, the aluminum precursor molarity was kept constant at 0.05 M, and the erbium molarity was varied from 0.005 M – 0.00025 M. Thus, our Al:Er 10:1 ratio is a high molarity erbium precursor with 200:1 being low molarity [15–18]. These Al:Er ratios will dictate the concentration of Er^{3+} ions encapsulated in the aluminum oxide nanoparticles. As will be discussed, these ratios also dictate the concentration of nanoparticles that are needed for power scaling in a fiber laser. Different synthesis techniques also were also investigated with the optimum one being carried out at 100°C, where the precursor salts were heated in a water bath, along with polyvinylpyrrolidone (PVP) surfactant, and 5 M NaOH was added dropwise until a pH of 9.5 was reached. The resultant suspension was a gel-like aluminum hydroxide phase, which subsequently was ripened in Teflon containers placed in an autoclave at 160 °C for 17 hours. After ripening, the suspension was centrifuged and washed 4 times in deionized (DI) water and then washed twice in methanol. In order to mitigate light scattering and refractive index variations in the preform core, it is important to avoid introducing NP agglomerates into the silica soot, so the surfactant polyvinylpyrrolidone (PVP) was used during synthesis. Agglomerates are virtually impossible to break up once they have formed in the dispersions.

The Ho-doped Lu_2O_3 nanoparticles were synthesized by co-precipitation of lutetium (III) nitrate hydrate (Sigma-Aldrich, 99.999%) and holmium chloride (Alfa-Aesar, 99.9%) precursors at a molar ratio of 25:1 in the presence of PVP heated to 100 °C. The pH was increased to a value of 9.6 by adding 5 M NaOH. The nanoparticles were then washed with 4 centrifugation steps of DI water and 2 with methanol. The resulting nanoparticles were dispersed in methanol using probe sonication.

Ho-doped and Er-doped LaF_3 nanoparticles were synthesized following the procedure given previously [7], where a fluorinated solution of NH_4F with Citric acid is prepared in a triple neck flask and placed in a hot bath at 70 °C. After the pH has been adjusted, the rare earth solution, either $Ho(NO_3)_3$ or $Er(NO_3)_3$, along with $La(NO_3)_3$ is then added into the fluorinated solution. The resultant dispersions were precipitated out of solution with the addition of ethanol. The resultant NPs were washed 4 times in DI water with centrifugation, and two with methanol, and the samples were dispersed in methanol.

Optics EXPRESS

The nanoparticle solutions were doped into the preform core in a manner similar to that used for solution doping, where the doping is performed *in situ* without having to remove the preform from the lathe. For preforms to be drawn into large core diameter fibers for a clad-pumped laser, multiple doping and consolidation steps were performed to achieve a multi-layer doped core. In all cases, after doping, the core experienced multiple drying stages, both in an oxygen environment and a chlorine environment, in order to remove solvent, residual OH, and surfactants. The doped soot preform was heat-treated with programmed temperature ramps and holds up to 1100 °C to remove residual solvent and OH, and to calcine the NPs, i.e., convert the aluminum hydroxide nanoparticle phase to alumina α-Al_2O_3:Er. However, we found that the temperature is high enough during preform consolidation and collapse to calcine the NPs, thus eliminating the need for a separate calcination stage.

Spatially-resolved Er luminescence and lifetime measurements were made on polished ~0.5 mm thick preform slices using a focused spot from a 980 nm laser for excitation and measuring the luminescence with an InGaAs detector. The spatial resolution was ~25 µm. Preform refractive index profiles were measured using a Photon Kinetics P104 profiler. Concentration profiles were measured on preform slices using electron microprobe analysis (EMPA); oxide compound and element weight percentages were determined, as were volume loadings. Fibers were drawn on a silica draw tower at a temperature of 2000 °C, and broadband spectral measurements 600 – 1700 nm were made using a Photon Kinetics FOA-2000 fiber measurement system. An Agilent 83437A EELED source and Ando AQ6315 OSA with 0.5 µm resolution were used to measure the Er peak absorption near 1530 nm, and spectral measurements in the 1650 – 2250 nm range were made with a Yokogawa AQ6375B long wavelength Optical Spectrum Analyzer and either a NKT SuperK COMPACT supercontinuum or an AdValue Photonics AP-ASE-2000 superluminescent source. Fiber refractive index profiles were measured with an Interfiber Analysis IFA-100 fiber index profiler.

Laser amplifier performance was evaluated for single mode erbium doped fibers with a core pumped master oscillator-power amplifier (MOPA) using a pump wavelength of 1476 nm (0 – 300 mW) and a 7 mW signal at 1560 nm. The pump and signal were combined in a wavelength division multiplexer whose output was spliced to the test NP doped fiber. A filter on the free-space MOPA output was used to separate the amplified signal from the unabsorbed pump. The slope efficiency was determined by linearly fitting the output power versus absorbed pump measured at each length as the fiber was cut back; the launched power was measured by cleaving the Er-doped laser fiber shortly after the splice with the SMF.

Clad-pumped laser investigations were performed using double clad (DC) erbium NP doped fiber with an octagonal-shaped pump cladding to enhance mode overlap and avoid doughnut modes. The core diameter was increased by depositing multiple core layers using multiple nanoparticle doping and consolidation steps. The target core and cladding flat-to-flat diameters were 20 and 125 µm, respectively, to match the dimensions of the passive components in the test setup. However, the actual drawn core diameter was 23 µm and the cladding flat-to-flat distance was 127 µm, which caused some splice loss. The glass fiber was coated with a low refractive index polymer to provide a pump cladding NA = 0.46. The laser set-up is shown schematically in Fig. 1. The fiber was resonantly pumped at 1532 nm using a commercial Er

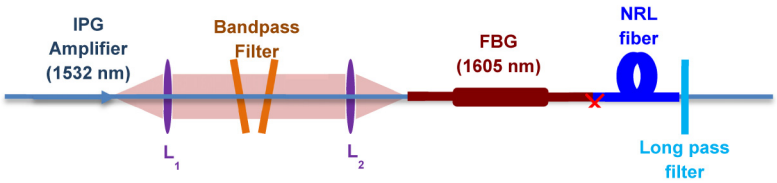

Fig. 1. Laser measurement set-up for resonantly clad-pumped Er NP doped fiber.

Optics EXPRESS

doped fiber amplifier (IPG) seeded at 1532 nm. A 1605 nm fiber Bragg grating with a reflectivity of 99.5% was spliced onto the end of the test fiber and a bandpass filter was used to isolate the pump source from backward propagating power of the tested fiber laser. Subsequent laser testing was done using a wavelength non-selective mirror in place of the fiber Bragg grating.

The holmium NP doped single-mode fibers were resonantly core-pumped by a single mode 1.95 µm thulium doped fiber laser pump; the laser cavity was formed by a 2.09 µm high reflector fiber Bragg grating and the 4% Fresnel reflection of the cleaved fiber end. A dichroic mirror was used to split the residual pump and signal power, and the cutback method was used to determine efficiency versus fiber length.

3. Results and discussion

3.1 Nanoparticle doping with erbium

Several NP ripening schedules were investigated in this work; initially, the schedule published by Pastouret [4] of 1 week at 95 °C was employed but this led to NP dispersions with significant agglomeration consisting of both pink and white layers. These layers are evidence of non-uniformity in the erbium NP doping levels. The TEM image shown in Fig. 2(a) clearly shows the platelet structures that are attributable to Er-doped boehmite Er:AlOOH, as well as rod-like structures which are not identified. The XRD data show no evidence of boehmite but clear evidence of a different Al hydroxide phase Bayerite, which is seen in both the white and pink precipitate layers. As shown in Fig. 2(b), hydrothermal ripening for 1 week at 160 °C once again resulted in agglomeration and precipitation of white and pink material. XRD has identified Boehmite, erbium oxide and erbium-aluminum oxide phases; the Boehmite platelets are seen in the TEM image in addition to the rods attributable to the other phases.

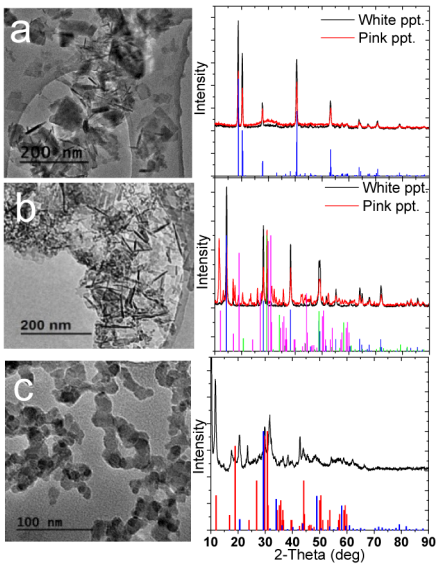

Fig. 2. TEM and corresponding XRD patterns for various phases of Er aluminum doped nanoparticles synthesized in this work. a.) blue peaks correspond to bayerite $Al(OH)_3$ b.) blue peaks correspond to boehmite AlOOH, green to Er_2O_3, pink to $Er_4Al_2O_9$ c.) red peaks correspond to $Er_4Al_2O_9$, blue to Er_2O_3. The pink and white layers of precipitate are described in the text.

The agreement is quite good between the XRD data and Boehmite and erbium-aluminum oxide references but only weak with erbium oxide.

Optics EXPRESS

A schedule of 17 h at 160 °C was ultimately found to be preferable as it resulted in a dispersion that appears to contain erbium oxide and erbium aluminum oxide, as shown in Fig. 2(c). It is worth noting, however, that the agreement between the data and reference is not as convincing as in the other ripening cases, perhaps due to the small NP size and the presence of amorphous material. However, the XRD data did not exactly correspond to any other reference phases containing Er, Al and O. Ripening for 17 h at 160 °C was found to produce the most stable dispersions with only a small amount of precipitation. Although the ripening conditions obviously affect the nanoparticle size and morphology, it is important to note that any Al-oxide phase formed is able to equally encapsulate the erbium ions. Furthermore, the soot consolidation and preform collapse stages are at temperatures of 1700-2000 °C, so any oxide phases are converted to Er-doped Al_2O_3 [15–18].

Proper selection of surfactant, synthesis temperature and pH, has kept agglomeration to a minimum, which is critical for obtaining smooth refractive index profiles and reducing scattering of light. An example of this is given in Fig. 3 where a representative preform refractive index profile and corresponding spatially-resolved luminescence intensity are provided. It is evident the Er^{3+} ions are well distributed throughout the preform core using nanoparticle doping. A major accomplishment of this effort is the development of a method for incorporating large concentrations, to ~4 wt% nanoparticles into the SiO_2 matrix, as determined by EMPA.

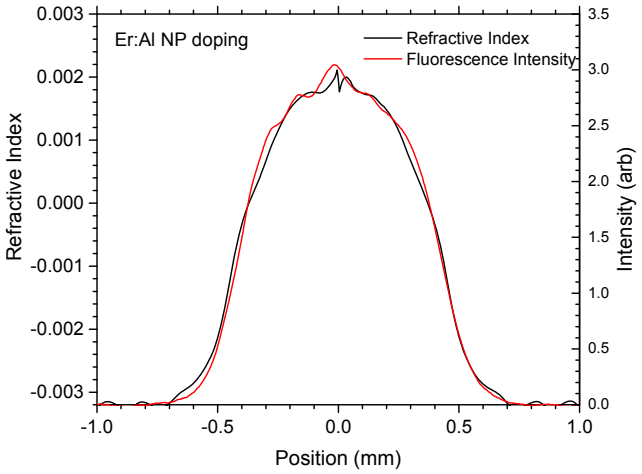

Fig. 3. Refractive index profile and corresponding fluorescence intensity profile for a Er:Al nanoparticle doped preform.

The measured fluorescence lifetime (at the 1/e point) as a function of normalized intensity for more than 35 NP-doped samples, and a comparison to solution-doped preforms is given in Fig. 4. Measured lifetimes as long as 11.7 ± 0.1 ms have been observed in Er:Al_2O_3-doped preforms, which represents a 10% increase over those for solution doping, and there is a general trend of longer lifetimes for the same fluorescence intensity (corresponding to Er concentration) in the Er:Al_2O_3 NP-doped samples vs. solution-doped samples. These results indicate that excited state energy transfer mechanisms usually causing lifetime quenching have been reduced relative to glass prepared by conventional solution doping techniques. Also presented in Fig. 4 are results for Er:LaF_3 nanoparticle doped preforms. In this case the lifetimes are comparable to solution doped preforms.

Optics EXPRESS

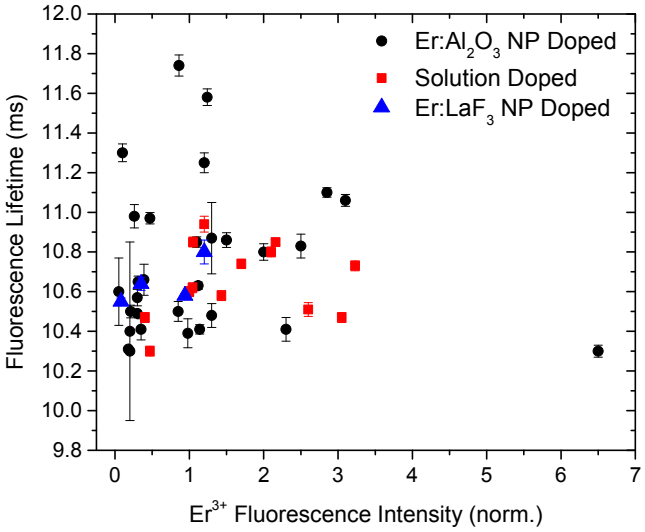

Fig. 4. Fluorescence lifetime as a function of fluorescence intensity for Er nanoparticle and solution doped preform samples.

Our optical absorption measurements have indicated that Er peak absorption values greater than 90 dB/m at 1532 nm can be realized, which corresponds to concentrations of about 6.41 x 10^{25} ions/m^3, as confirmed by EMPA. The drawn NP doped fibers possess low background losses, on the order of < 40 dB/km at 1300 nm, and, despite the NPs being formed using an aqueous process extremely low OH concentrations of ~0.3 ppm are obtained in the resultant fibers as measured from the second OH overtone band at 1380 nm [16,17].

The slope efficiency for several resonantly-pumped single-mode Er-NP-doped fibers is plotted as a function of Er^{3+} peak absorption in Fig. 5. Also included in Fig. 5 is a typical absorption spectrum for an Er:Al_2O_3 NP doped fiber (emission cross sections may be obtained from absorption data by using the McCumber relationship [3]). A slope efficiency (wrt absorbed power) of 74.4% has been demonstrated in a fiber with an Er^{3+} peak absorption of 22dB/m at 1530 nm. The Er^{3+} ion concentration determined by EMPA was 0.22 wt. % which yields an [Er] = 1.81x10^{25} ions/m^3. This is believed to be the highest slope efficiency reported for any erbium nanoparticle doped fiber. Furthermore, a slope efficiency of 46.3% has been maintained for doping levels up to ~63 dB/m (~4.37x10^{25} ions/m^3). Table 1 summarizes gain efficiency measurement results for resonantly pumped single-mode fiber amplifiers and lasing efficiency of the clad-pumped DC fibers in a power oscillator configuration with the Er-NP doped cores. The latter fibers had an octagonally shaped pump cladding and are marked as "DC" in the Table. The fiber core and clad diameters are given as well as the test method. An image of the octagonal end-face of a DC fiber is given in Fig. 6.

Optics EXPRESS

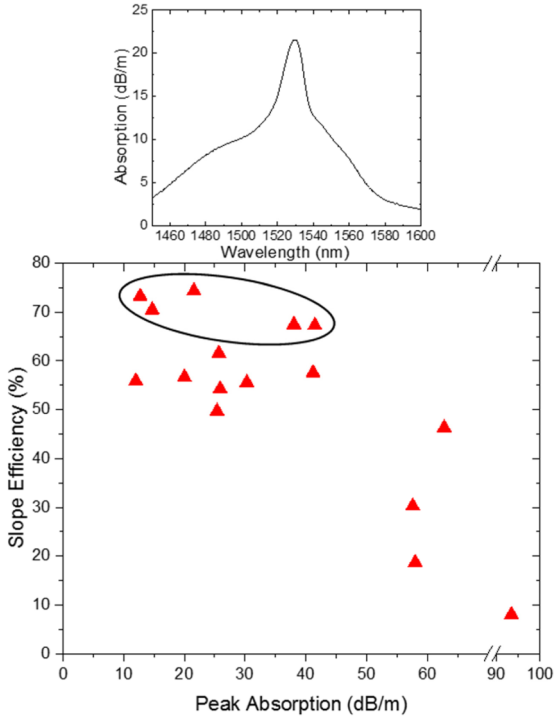

Fig. 5. Absorption spectrum for a Er:Al_2O_3 NP doped fiber and slope efficiency for NP-doped fibers vs. peak Er^{3+} absorption at 1532 nm. Precursor Al:Er ratios of 50:1 are circled.

The highest efficiency occurred for a ratio of Al:Er precursor molarities of 50:1. This ratio represents a low molarity erbium precursor, highlighted in the figure by the circled data points. As discussed, increased Er^{3+} concentrations are required for high power lasing, both to minimize the active fiber length to reduce nonlinear processes and because of the areal dilution in cladding-pumped configurations. Using low molarity dispersions requires very high loadings of nanoparticles in the fiber. Earlier attempts at increasing the concentration of erbium in the fibers were focused on increasing the Er precursor molarity (while maintaining the same Al molarity, thus decreasing the Al:Er ratio) where solutions with Al:Er of 20:1 or 10:1 were used. These lower ratios lead to lower slope efficiencies because the erbium concentration in the precursor solution was too high. This could have several detrimental effects during synthesis, such as the formation of clusters of erbium within the NP host, or the formation of separate erbium oxide nanoparticles along with Al-OH nanoparticles as shown in Fig. 2. By decreasing the amount of erbium in the precursor, to a ratio of 50:1, there is a better opportunity to encapsulate and isolate erbium ions so that they do not suffer these detrimental effects.

Table 1. Slope efficiencies and properties of Er^{3+}:NP doped fibers. Gain and laser measurements were done with either a core pumped MOPA (for single mode fibers) or clad pumped power oscillator configuration. The latter were used with either Bragg grating or high reflectivity mirror (HRM) as a pump-end mirror.

NRL fiber	Core/clad dia.	NP Host	Er Abs (dB/m)	Er conc (#/m^3)	pump	Test Method	Slope efficiency
161014	9.4/145	Al_2O_3	22	$1.81x10^{25}$	core	MOPA Core, gain	74.4%
161109	7.8/150	Al_2O_3	38	$2.22x10^{25}$	core	MOPA Core, gain	67.5%
160823	20/125 DC	Al_2O_3	0.9*	$1.57x10^{25}$	clad	Clad pump laser, HRM	49.2%
161205	23/127 DC	Al_2O_3	0.8*	$2.49x10^{25}$	clad	Clad pump laser, Bragg	53.0%
151216	10/125	LaF_3	10.75	$4.27x10^{24}$	core	MOPA Core, gain	71.4%

Optics EXPRESS

Ideally, the highest ratio of Al:Er possible would be needed to completely ensure the isolation of RE^{3+} ions within the nanoparticle host. Boivin, et al., determined that a ratio for Al:Er precursor concentration as high as 350:1 is needed [5]. A ratio of 50:1 Al:Er ratio represented a compromise between the maximum concentration of nanoparticles that can be incorporated into the silica soot without devitrification and being able to incorporate as many erbium ions as possible for lasing. While this ratio results in a relatively high concentration of aluminum in the fiber, the concentration is still lower than for solution doping [16].

The highest slope efficiency NP doped sample had an Al:Er ion ratio of ~50 in the preform; in contrast, a typical solution doped preform may have a Al:Er ion ratio of >150. These concentrations are important for waveguide control since increased Al_2O_3 concentrations results in high refractive index, which will compromise single mode waveguiding in large mode area fibers (or require complicated pedestal structures). Furthermore, the Er ions in a solution-doped core with a ratio of Al:Er as low as in the NP doped glass would be highly quenched. There is much less excess Al in NP-doped fibers because the only Al incorporated into the preform is through Al-O nanoparticles [16].

Results for clad pumped lasing of a Er:Al_2O_3 NP fiber are presented in Fig. 7, and Clad pumped lasing results are also summarized in Table 1. A slope efficiency (wrt absorbed power) of 53% was measured for this fiber. It is important to note that there is significant loss at the 1532 nm pump wavelength due to absorption in the low index polymer coating used as the pump cladding. These low index coatings are designed for use with Yb-doped fiber lasers, generally to be pumped near 975 nm, but there are significant absorptions >1100 nm, and we have measured the loss at 1532 nm to be 0.08 dB/m. When the polymer loss is taken into account, the slope efficiency of the Er-NP-doped fiber laser increases to 59%, as shown in Fig. 7.

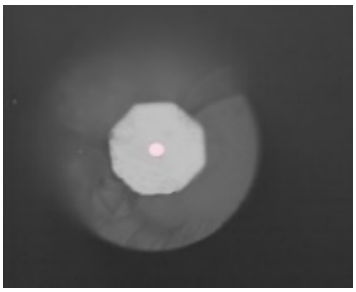

Fig. 6. Er doped NP containing fiber with an octagonal pump cladding. The core/clad diameters are 23/127 μm.

Further improvement could be achieved with either an air-clad design or improved polymer coatings of lower absorption. Note that the slope efficiency of an Er-NP-doped single mode fiber made with a similar NP dispersion measured in a single-mode core-pumped MOPA was 67%, so the clad pumped results are quite encouraging, especially considering the splice loss. To our knowledge this is the first demonstration of efficient clad-pumped lasing in an erbium nanoparticle doped fiber.

Optics EXPRESS

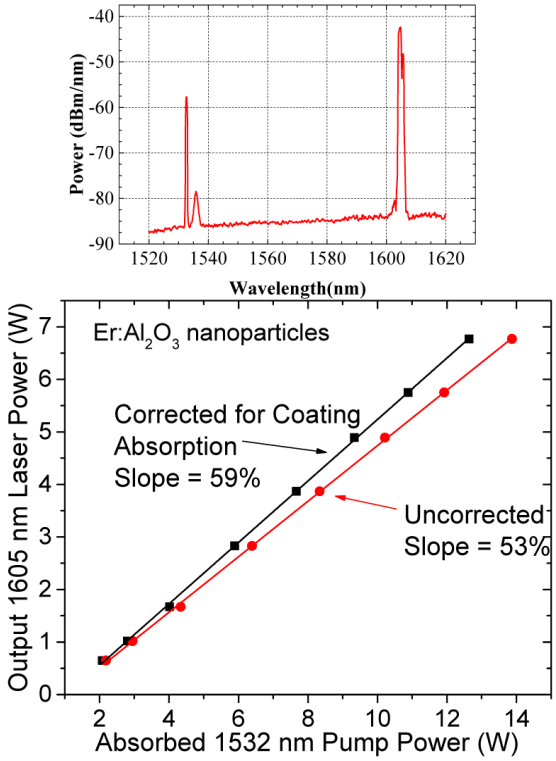

Fig. 7. Er:Al_2O_3 NP laser spectrum and slope efficiency of a resonantly-pumped, dual clad Er doped NP containing fiber with an octagonal pump cladding.

3.2 Nanoparticle doping with holmium

As discussed above, multiphonon lifetime quenching is a significant issue for Ho-doped silica fibers due to the relatively large phonon energy of the silica matrix. Encapsulating the Ho^{3+} ions in a NP of low phonon energy might be a way to shield the ion from the silica matrix, thereby reducing quenching. Initial efforts with holmium NP doping have included both Ho:LaF_3 and Ho:Lu_2O_3 NP systems, as both are low phonon energy hosts. We note that the fluorine nanoparticle hosts are converted to oxide during preform processing, however lanthanum contributes to a reduced phonon energy [7]. Lifetime measurements were performed on polished preform samples ~3 cm in length using a nanosecond 1.95 μm pump and detection from the side of the preform through a 2120 nm filter with 100 nm bandpass. Results on lifetime and slope efficiencies are provided in Table 2, along with core and clad diameters and Ho^{3+} ion concentrations. Measurements on both Ho^{3+} solution doped and the Ho:LaF_3 NP preforms indicate that there is a small increase of up to 33% in lifetime with NP doping. However, these improved lifetime values are still far lower than those predicted based on Judd-Ofelt analysis [14]. The LaF_3 disassociates and reacts with the silica as described above and in Ref. 19, so the Ho^{3+} is not likely as well shielded from the silica matrix. The Ho:Lu_2O_3 NP-doped samples exhibited too much pump scatter for measurement, but this system may show even more improved lifetime results in our future efforts to reduce the scatter.

Optics EXPRESS

Table 2. Measured luminescent lifetimes and properties of the NP- and solution-doped samples. **Excessive scattering

NRL fiber	Core/clad dia.	NP host	Lifetime (ms)	Ho Abs. (dB/m)	Ho Conc. (#/m^3)	Slope Eff.
161101	10/111	solution	0.62	51	$3.66x10^{25}$	60-80%
161129	10/123	LaF_3	0.83	26	$2.86x10^{25}$	82.3%
160706	10.5/125	LaF_3	0.68	42	$4.51x10^{25}$	62.5%
160816	9.9/125	LaF_3	0.74	97	$9.18x10^{25}$	30.0%
161221	10/100	Lu_2O_3	**	7	$1.29x10^{25}$	85.2%

Drawn fibers using the Ho-doped NPs exhibited background losses as low as 20 dB/km at 1450 nm, and the intensity of the second Si-OH overtone band at 1380 nm indicates that OH concentrations of <0.5 ppm were achieved. Figure 8 shows the Ho^{3+} absorption in the 2 µm wavelength region; in other measurements that extend beyond 2200 nm, there is an absence of any significant absorption at 2210 nm from the Si-O-H combination band since the OH concentration was so low.

Figure 8 verifies that pumping at a wavelength of 1.95 µm is ideal for laser measurements since the peak of the Ho^{3+} absorption is excited and there is very little absorption at the laser wavelength of 2.09 µm. Cutback measurements were made to obtain the maximum slope efficiency for the Ho:LaF_3 single mode nanoparticle doped fiber shown in Fig. 9. The Ho^{3+} absorption peak for this fiber was measured to be 26.25 dB/m, corresponding to a Ho3+ ion concentration of 2.86 x 1025 ions/m3, and the maximum slope efficiency was measured to be 82.3%, as shown in Fig. 9.

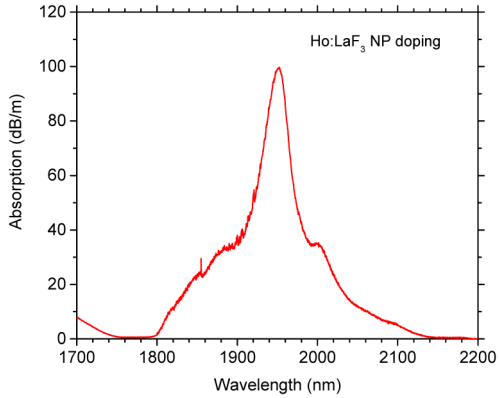

Fig. 8. Absorption spectrum for Ho:LaF_3 nanoparticle doped fiber.

Although there was excessive scatter in the Ho:Lu_2O_3 nanoparticle doped preform, the background loss in fiber drawn from this preform was only 16 dB/km. This difference could be due to the rapid thermal quenching that occurs during fiber drawing preventing the formation of scattering centers. The slope efficiency measured in this fiber was very high, 85.2%, as shown in Fig. 9. This fiber had a holmium absorption peak measured to be 7 dB/m at 1950 nm, corresponding to a Ho^{3+} ion concentration of 1.29 x 10^{25} ions/m^3. These results are very encouraging, as they represent the first demonstration of lasing in Ho:NP-doped fibers. Future efforts will focus on approaches to increase the holmium concentration in the fiber while maintaining high slope efficiency.

Optics EXPRESS

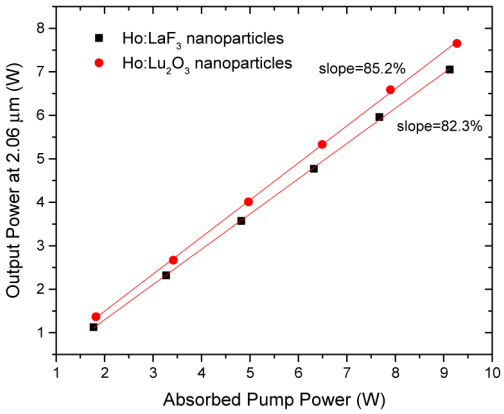

Fig. 9. Ho:LaF_3 NP doped fiber with an optical-to-optical slope efficiency of 82.3% and a Ho:Lu_2O_3 NP doped fiber with an optical to optical slope efficiency of 85.2% at a wavelength of 2.09 µm.

4. Conclusion

We have shown that nanoparticle doping is an effective method for reducing excited state energy transfer processes, as well imparting unique materials properties. Erbium nanoparticle doped fibers have longer fluorescence lifetimes than those that are solution doped, indicating that the Er^{3+} ions are in a more favorable location by being surrounded by aluminum in the fiber core. Using a core-pumped MOPA we have measured an optical to optical slope efficiency of 74.4% in an NP doped fiber which had an erbium ion concentration corresponding to an absorption of 22 dB/m (1.81 x 10^{25} ions/m^3). Our efforts at using low erbium precursor concentrations with higher nanoparticle loadings have allowed the Er^{3+} ions to be more successfully encapsulated in the aluminum oxide matrix, thus ensuring higher efficiencies at increased concentrations. We have demonstrated what we believe to be the highest output power and highest efficiency pumped laser using Er nanoparticles with a measured slope efficiency of 53%, reduced by the absorption of the low refractive index commercial polymer coating on the pump cladding.

We have successfully demonstrated Ho^{3+} nanoparticle doped fibers, and shown what we believe to be the first ever demonstration of lasing in these materials. The Ho^{3+} doped LaF_3 NP fiber showed a slope efficiency of 82.3%, and the Ho^{3+} doped Lu_2O_3 NP fiber had an efficiency of 85.2%. Future efforts will include maintaining high efficiency with increased nanoparticle loadings.

Funding

High Energy Laser Joint Technology Office (13-S&A-0514, 15-S&A-0553); Office of Naval Research/Naval Research Laboratory; J. E. Sirrine Foundation.

Acknowledgements

The authors acknowledge the technical contributions of Charles Askins, Fred Kung, Barbara Marcheschi, John Peele, and Michael Hunt.